
FlexSelect: Flexible Token Selection for Efficient Long Video Understanding

Yunzhu Zhang^{1*†} Yu Lu^{1†} Tianyi Wang² Fengyun Rao²
Yi Yang¹ Linchao Zhu^{1‡}

¹The College of Computer Science and Technology, Zhejiang University

²WeChat Vision, Tencent Inc.

Abstract

Long-form video understanding poses a significant challenge for video large language models (VideoLLMs) due to prohibitively high computational and memory demands. In this paper, We propose **FlexSelect**, a flexible and efficient token selection strategy for processing long videos. FlexSelect identifies and retains the most semantically relevant content by leveraging cross-modal attention patterns from a reference transformer layer. It comprises two key components: (1) a **training-free token ranking pipeline** that leverages faithful cross-modal attention weights to estimate each video token’s importance, and (2) a **rank-supervised lightweight selector** that is trained to replicate these rankings and filter redundant tokens. This generic approach can be seamlessly integrated into various VideoLLM architectures, such as LLaVA-Video, InternVL and Qwen-VL, serving as a plug-and-play module to extend their temporal context length. Empirically, FlexSelect delivers strong gains across multiple long-video benchmarks – including VideoMME, MLVU, LongVB, and LVBench. Moreover, it achieves significant speed-ups (*e.g.*, up to $9 \times$ on a LLaVA-Video-7B model), highlighting FlexSelect’s promise for efficient long-form video understanding. Project page: https://yunzhuzhang0918.github.io/flex_select.

1 Introduction

Long-form video understanding is crucial for applications such as analyzing movies, building multimodal web agents [26], assisting in video surveillance tasks. Recent Video Large Language Models (VideoLLMs) [1, 47, 6, 21, 49, 41, 19] have shown impressive results on short video clips, combining vision and language processing to answer questions or follow instructions about video content. However, extending these models to process long videos presents significant challenges. Long videos yield a substantial volume of visual tokens, often surpassing the context length of transformer-based LLMs. Additionally, processing entire long videos with VideoLLMs leads to excessive computational and memory overhead, making effective long video analysis infeasible.

To mitigate this, some recent works [8, 27] employ training-based compression modules [16, 45] to summarize visual tokens into a compact representation via finetuning on long-video datasets. However, these methods introduce substantial overhead due to additional training. Alternatively, other approaches [12, 29] leverage cross-modal attention scores from pre-trained VideoLLMs to rank and prune video tokens without training. While more efficient, these attention-based heuristics often

*Work done during internship at Wechat Vision.

†Equal Contribution.

‡Corresponding Author.

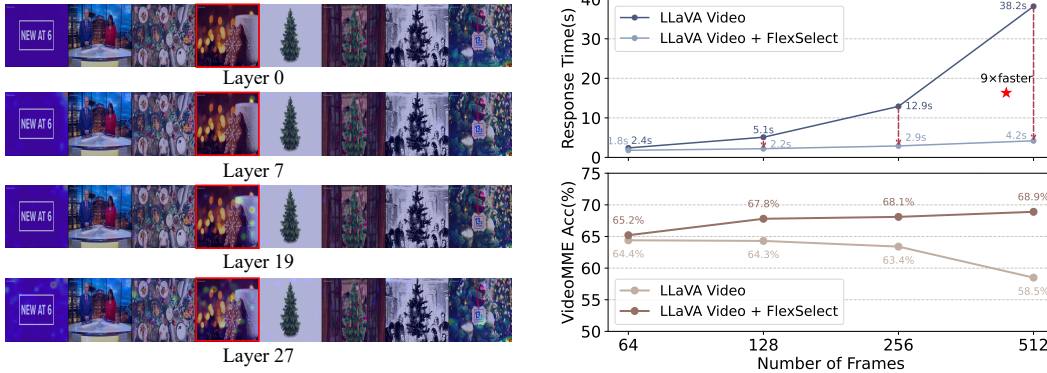


Figure 1: (a) Visualization of cross-modal attention maps of LLaVA-Video-7B across layers (user query : "what's the color of the cup?"). Attention scores progressively highlight the query-related regions (the cup) with layer depth, and this highlighting is most pronounced at the specific **reference layer** (layer 19 in example). FlexSelect employs attention scores from this layer to select semantically related visual tokens. (b) VideoMME accuracy and response time (time to generate the first token) of LLaVA-Video-7B. The original model with 64 input frames achieves limited accuracy 64.4% due to inadequate coverage for long video content, while increasing frames will overload the model's context window, reducing accuracy to 58.5% and slowing response time to 38.2s. FlexSelect improves this by filtering irrelevant tokens, achieving 68.9% accuracy at 512 frames with 9x faster response (4.2s).

suffer from performance degradation due to inconsistent relevance patterns across transformer layers, which may not reliably reflect the semantic importance of visual tokens for the task.

In this paper, we present **FlexSelect**, a general-purpose framework for efficient long-form video understanding. FlexSelect enables VideoLLMs to **focus on the semantically relevant visual tokens for the query** by identifying and filtering out less informative visual tokens before heavy multimodal reasoning occurs. Crucially, FlexSelect is **architecture-agnostic** and does not require any modifications or training of the base VideoLLM. It acts as a preprocessor that significantly extends the model's effective temporal context window without compromising its reasoning ability.

A central observation underlying FlexSelect is that well-trained VideoLLMs inherently encode meaningful cross-modal relevance signals within their internal attention maps. In particular, the cross-attention weights between textual queries and visual tokens progressively reflect semantic alignment across transformer layers and typically peak at an intermediate depth (Fig. 1(a)). Motivated by this, FlexSelect extracts attention scores from an empirically identified *optimal reference layer* to derive **faithful, training-free token importance rankings**. These scores enable the selection of semantically critical visual tokens while discarding redundant or irrelevant ones, thus substantially reducing token volume without compromising the model's reasoning capability. Unlike existing methods that rely on extensive training or oversimplified heuristics, FlexSelect dynamically balances efficiency and performance by exploiting the latent structure of attention patterns within VideoLLMs.

To reduce the computational cost of processing long videos with VideoLLM layers for token ranking, we introduce **a lightweight selector network** trained to mimic the reference layer's ranking. The selector is supervised with a ranking loss and learns to assign higher scores to tokens that the reference model would attend to. This allows for flexible token selection without retraining the full model. Once trained, it efficiently selects the top-ranked visual tokens from long videos, significantly reducing computational overhead. These tokens are then passed into original VideoLLM for final reasoning. In doing so, FlexSelect replicates large model's attention patterns at a fraction of the computational cost.

FlexSelect is a generic approach can be seamlessly integrated into various VideoLLM architectures, such as **LLaVA-Video, InternVL and Qwen-VL**. FlexSelect serves as a plug-and-play inference module requiring no changes to the base VideoLLM. We evaluate it on four challenging long-video understanding benchmarks—VideoMME, MLVU, LongVB, and LVBench—using VideoLLMs of varying sizes, from 7B to 72B parameters. Experimental results show that FlexSelect achieving significant speed-ups (e.g., up to 9x faster inference with LLaVA-Video-7B) while maintaining or

improving performance. Notably, by filtering out irrelevant content, FlexSelect not only accelerates inference but enhances final answer quality.

Contributions. To summarize, our contributions are threefold:

- We propose **FlexSelect**, a flexible and architecture-agnostic framework that extracts faithful cross-modal token relevance from an optimal reference layer in VideoLLMs to select semantically important visual tokens for long-form video understanding.
- We design a **lightweight rank-supervised selector** that mimics the cross-modal attention ranking from a reference model layer, enabling fast and accurate token filtering without modifying or retraining the base VideoLLM.
- We demonstrate that FlexSelect is a generic framework applicable to various VideoLLMs, achieving **up to 9× speed-up** and improved accuracy on four long-video benchmarks across multiple model scales.

2 Related Works

Long-form Video Understanding Current VideoLLMs showcase remarkable video-language understanding abilities. However, it is still challenge to process long-form videos due to the extensive visual tokens. Recent approaches mainly address this by two ways: (1) applying length extrapolation methods (e.g. YARN [25]) to VideoLLMs and training on longer sequences [5, 43] to support long context input. (2) adopting trainable compression modules to VideoLLM to compress visual content into fewer tokens [10, 18, 27, 8, 13] via post-finetuning. Different from these approaches, we introduce a token selector to directly select semantically relevant visual tokens before LLM generation, without training the large-scale VideoLLM, which is more efficient.

Attention-based Token Pruning Recent works explore visual token pruning for efficient image-text understanding using cross-modal attention scores. FastV [4] first identifies visual token inefficiency in LLM processing, pruning tokens via second-layer attention scores but suffering significant accuracy drops. PyramidDrop[37] observes increasing redundancy with layer depth, applying predefined layer-wise drop ratios to prune more tokens at deeper layers for better results. SparseVLM [46] dynamically adjusts pruning ratios through attention score ranks at each layer, improving performance yet still suboptimal. Recently, FrameFusion [12] and Dycok [29] analyse redundancy in video data [34], applying similar attention-based token pruning methods to VideoLLMs, improving efficiency but also degrading performance. Meanwhile, several studies [44, 35, 9] show that attention scores fail to reliably indicate semantical relevance of visual tokens because of the attention shift phenomenon, where later tokens tend to have a higher scores due to the autoregressive characteristic of LLM. However, these conclusion are limited because they only discuss layer-averaged attention scores. In this paper, we conduct comprehensive layer-wise analysis on the cross-modal attention pattern, and identify a reference layer where attention scores can reliably indicate the semantical relevance of visual tokens.

3 Methods

We present **FlexSelect**, a token selection strategy for long-form video understanding. FlexSelect consists of two complementary components: (1) a **training-free selection pipeline** that leverages faithful cross-modal attention scores in VideoLLM to select semantically relevant visual tokens from a long video, and (2) a **lightweight rank-supervised model** trained to replicate the visual token rankings of the faithful cross-modal attention scores from VideoLLM. This section first analyzes token semantic relevance across transformer layers to identify the reference layer, then explains the training-free FlexSelect procedure for long video understanding, and finally details the rank-supervised token selector, covering its architecture, training objective, and integration into the framework.

3.1 Layer-wise Semantic Relevance Analysis

VideoLLMs employ transformer decoder to process video frames as sequences of visual tokens. However, not all tokens are equally relevant to a given query. To identify which decoder layer

best captures **semantic relevance**, we perform a layer-wise analysis using a “*needle-in-haystack*” experiment. Specifically, we insert one unique **needle frame** (image containing distinctive visual content) at random positions in a video sequence. We design a query solely about the needle image so that the visual tokens derived from it are treated as ground-truth *semantically relevant tokens*, while all other tokens are considered irrelevant. By passing the augmented video through the VideoLLM and analyzing the attention patterns at each layer, we assess whether the model successfully highlights these needle visual tokens as semantically aligned with the query.

For a given transformer layer l , let $r_i^{(l)}$ denote the *semantic relevance score* of visual token i at that layer. We derive $r_i^{(l)}$ from the model’s cross-modal attention. Formally, if $A_{q \rightarrow i}^{(l,h)}$ is the attention weight from query tokens q to visual token i in head h of layer l , then:

$$r_i^{(l)} = \frac{1}{H} \sum_{h=1}^H A_{q \rightarrow i}^{(l,h)}, \quad (1)$$

where H is the number of attention heads. This score reflects how strongly the model semantically links visual token i to the query. We rank all visual tokens by $r_i^{(l)}$ in descending order to produce a semantic relevant ranking at that layer.

To quantify how faithfully each layer’s semantic relevance scores identify the ground-truth semantically relevant tokens (the needle visual tokens), we use the Recall@K metric, which computes the fraction of relevant tokens recovered in the top- K ranked tokens. Denote $\text{TopK}(l)$ is the set of top- K tokens ranked by $r_i^{(l)}$, and R is the set of needle visual tokens considered semantically relevant by construction, then:

$$\text{Recall@K}(l) = \frac{|\text{TopK}(l) \cap R|}{|R|}, \quad (2)$$

We evaluate Recall@K for each transformer layer l by choosing $K = |R|$ (so that perfect recovery of all needle visual tokens in the top- K yields $\text{Recall@K} = 1.0$). A higher Recall@K indicates that the layer’s relevance is more faithful to the query.

Results of Layer Analysis: Figure 2 illustrates the Recall@K value across all transformer layers in the LLM decoder of LLaVA-Video-7B. We observe substantial variation in the effectiveness of different layers at retrieving semantically relevant tokens. Specifically, early layers exhibit relatively low Recall@K scores, suggesting that the attention distributions at these stages are less aligned with the semantic relevance of the query. Very deep layers also not highlight the needle frames as the model has already consolidated the critical visual information into the final token for next token generation. Interestingly, an intermediate layer achieves the highest Recall@K, indicating that it best identifies the target visual tokens among its top-ranked outputs. In other words, L_{ref} serves as the optimal attention layer that most reliably captures truly semantic-relevant tokens in the sequence. Based on this finding, we designate layer L_{ref} as the reference layer for guiding token selection in FlexSelect. All subsequent token semantic-relevance computations in our method will use the reference layer’s attention scores as the measurement of semantic importance. More analysis including more base models and PCA visualization on tokens can be found in appendix A.1.

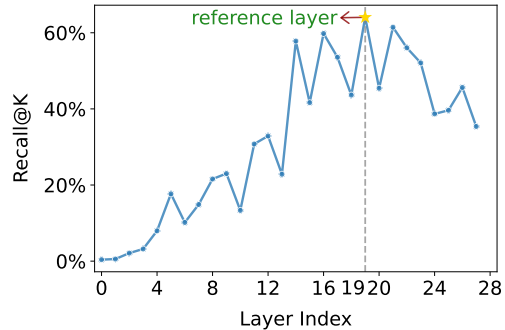


Figure 2: Recall@K values across different layers in LLaVA-Video-7B. Recall@K metric is the recall ratio of ground-truth relevant tokens (e.g., needle-frame tokens) among the top-K tokens ranked by a layer’s cross-modal attention scores. A higher Recall@K indicates the attention scores of that layer can more accurately identify the semantically related visual tokens. We choose the optimal layer with the highest Recall@K as the reference layer for token selection.

3.2 Training-Free FlexSelect Pipeline

Even with the reference layer L_{ref} identified, processing a long video in a single forward pass is typically infeasible due to the quadratic cost of self-attention and memory constraints. To address

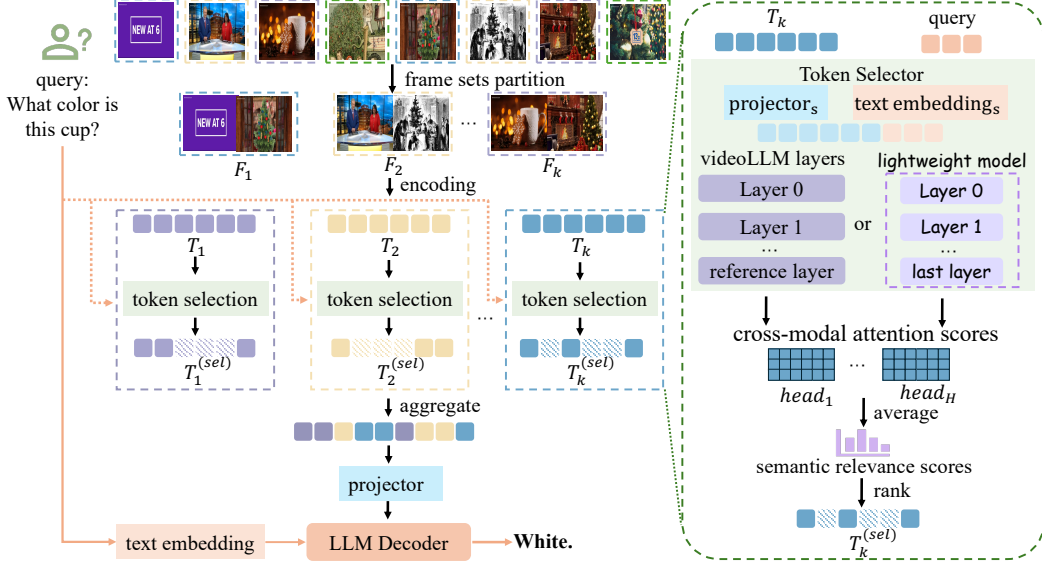


Figure 3: **Overview of FlexSelect token selection pipeline.** Given a long video and a query, FlexSelect first partitions the video into frame sets and encodes each into visual tokens. For each set, a token selector identifies semantically relevant tokens by ranking cross-modal attention scores from a reference layer in a pre-trained VideoLLM or a lightweight selector network trained to approximate it. In this process, the projector_s and text embedding_s are employed to convert the visual tokens and user queries into tokens that match the dimension of subsequent transformer layers. After getting the scores, the top-ranked tokens across all segments are aggregated and projected into the decoder for final reasoning. FlexSelect operates in a training-free or rank-supervised mode, and serves as a plug-and-play module that enables efficient long-video understanding without requiring modifications to the base VideoLLM.

this, we propose a training-free FlexSelect strategy that enables efficient visual token selection while preserving semantic coverage across the entire video. The video is divided into multiple *frame sets* uniformly, with token selection performed independently within each set. This approach ensures comprehensive temporal coverage without requiring the entire video sequence to be processed at once.

Frame Sets Partition. We partition the extensive frames into frame sets and each set most contains S frames to prevent token number exceeding the VideoLLM’s maximum context length. Given a video with N sample frames $\{f_1, f_2, \dots, f_N\}$, we construct $K = \lceil N/S \rceil$ *frame sets* $\{\mathcal{F}_1, \mathcal{F}_2, \dots, \mathcal{F}_K\}$ such that each set samples frames at a same stride. Formally, the j -th frame set is defined as $\mathcal{F}_j = \{f_i \mid i \equiv j \pmod N\}$, where $j \in \{1, \dots, K\}$. This sampling ensures that each frame set spans the entire video with different temporal offsets, capturing diverse temporal dynamics and reducing redundancy between sets.

Each frame set \mathcal{F}_j is encoded by the VideoLLM’s visual encoder. This yields a sequence of visual tokens $T_j = \{t_{j,1}, \dots, t_{j,M}\}$ for each set, M means the total number of visual tokens in a frame set.

Semantic Relevance Scoring and Token Selection. Within each frame set \mathcal{F}_j , we compute a semantic relevance score $r_{j,i}$ for each token $t_{j,i}$ using the attention mechanism at layer L_{ref} :

$$r_{j,i} = \frac{1}{H} \sum_{h=1}^H A_{q \rightarrow t_{j,i}}^{(L_{\text{ref}}, h)},$$

where $A_{q \rightarrow t_{j,i}}^{(L_{\text{ref}}, h)}$ is the attention weight from the query tokens q to token $t_{j,i}$ in head h , and H is the number of heads. This relevance score reflects the semantic alignment between each token and the query. We then rank the tokens in each T_j by $r_{j,i}$ and select the top- k tokens $T_j^{(\text{sel})} = \text{TopK}_k(\{r_{j,i}\})$, yielding a set of semantically relevant tokens for each frame set.

Aggregation and Final Token Composition. The selected tokens from all frame sets are aggregated to form the final visual token input $T_{\text{selected}} = \bigcup_{j=1}^K T_j^{(\text{sel})}$. This merged token set provides a globally informed yet compact representation of the video.

By constructing K frame sets with uniform sampling and processing them independently, our proposed FlexSelect strategy ensures that the framework scales efficiently to long video sequences. The method minimizes computational overhead by leveraging the parallelizability of processing smaller frame sets, while maintaining temporal fidelity across the video.

3.3 Rank-Supervised Lightweight Token Selector

While the training-free approach described above effectively reduces computational overhead, it still relies on partial forward passes through the large VideoLLM to score visual tokens. To further enhance inference efficiency, we introduce a *lightweight token selector* trained via rank supervision to predict semantic relevance scores independently. The selector model is explicitly designed to replicate the token-ranking behavior observed at the reference transformer layer L_{ref} .

Architecture and Input. Our lightweight token selector is a compact, shallow transformer-based network intended to substantially reduce inference costs compared to the large-scale VideoLLM. The model receives two inputs: visual tokens extracted by the vision encoder and the corresponding textual query. It outputs predicted semantic relevance scores for each visual token in the input sequence. Formally, for a visual token sequence $\{t_1, t_2, \dots, t_M\}$ paired with a textual query q , the selector produces scores $\{\hat{r}_1, \hat{r}_2, \dots, \hat{r}_M\}$ indicating each token’s predicted semantic alignment with the query. These scores are subsequently used to select the most relevant visual tokens, similar to the training-free method described above.

To leverage pretrained knowledge and accelerate training convergence, we initialize the selector from a smaller-scale pretrained VideoLLM (approximately 0.5B parameters). In our experiments, we separately train selectors for LLaVA-Video-7B, Qwen2.5VL-7B, and InternVL2.5-8B.

Rank-Supervised Training Objective. We train the lightweight selector with rank supervision, directly leveraging semantic relevance rankings provided by the reference transformer layer L_{ref} from the larger VideoLLM. For each training video-query pair, we first compute the semantic relevance scores $\mathbf{r}^{\text{ref}} = [r_1^{\text{ref}}, r_2^{\text{ref}}, \dots, r_M^{\text{ref}}]$ at the reference layer L_{ref} . Then, the lightweight selector predicts scores $\hat{\mathbf{r}} = [\hat{r}_1, \hat{r}_2, \dots, \hat{r}_M]$ for the same tokens.

The training goal is to align the predicted semantic relevance ranking $\hat{\mathbf{r}}$ with the reference ranking \mathbf{r}^{ref} . To quantify this alignment, we use the spearman rank correlation coefficient [28]:

$$\rho_{\text{spearman}}(\mathbf{r}^{\text{ref}}, \hat{\mathbf{r}}) = \frac{\sum_{i=1}^M (\text{rank}(r_i^{\text{ref}}) - \overline{\text{rank}(r^{\text{ref}})}) (\text{rank}(\hat{r}_i) - \overline{\text{rank}(\hat{\mathbf{r}})})}{\sqrt{\sum_{i=1}^M (\text{rank}(r_i^{\text{ref}}) - \overline{\text{rank}(r^{\text{ref}})})^2 \sum_{i=1}^M (\text{rank}(\hat{r}_i) - \overline{\text{rank}(\hat{\mathbf{r}})})^2}}. \quad (3)$$

$\rho_{\text{spearman}}(\mathbf{r}^{\text{ref}}, \hat{\mathbf{r}})$ closer to 1 indicates stronger consistency between the ranking orders of \mathbf{r}^{ref} and $\hat{\mathbf{r}}$, while closer to 0 suggests no monotonic relationship. The corresponding training loss is defined as:

$$\mathcal{L}_{\text{rank}} = 1 - \rho_{\text{spearman}}(\mathbf{r}^{\text{ref}}, \hat{\mathbf{r}}). \quad (4)$$

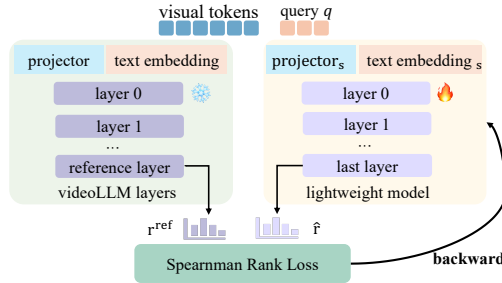


Figure 4: Illustration of our rank-supervised training. We align lightweight model’s predicted scores $\hat{\mathbf{r}}$ with the reference layer’s semantic relevance scores \mathbf{r}^{ref} by optimizing the spearman rank correlation coefficient between them. Once trained, the ranking derived from these two scores will follow similar order, enabling the lightweight model to rank the visual tokens as the reference layer does and select the related tokens quickly.

Model	Size	VideoMME		MLVU	LongVB	LVBench
		Long	Overall	M-Avg	Val	Test
Proprietary Models						
GPT-4o [24]	-	65.3	71.9	64.6	66.7	34.7
Gemini-1.5-Pro [30]	-	67.4	75.0	-	64.0	33.1
Open-Source VideoLLMs						
mPLUG-Owl3 [39]	7B	50.1	59.3	63.7	52.1	43.5
Qwen2-VL [32]	7B	53.8	63.3	66.9	55.6	42.4
NVILA [21]	8B	54.8	64.2	70.1	57.7	-
VideoLLaMA3 [40]	7B	-	66.2	73.0	59.8	45.3
Aria [15]	8x3.5B	58.8	67.6	70.6	65.3	-
Oryx-1.5 [22]	34B	59.3	67.3	72.3	62.0	30.8
Video-XL-Pro [20]	3B	-	60.0	70.6	56.7	-
SF-LLaVA-1.5 [38]	7B	-	63.9	71.5	62.5	45.3
TPO [17]	7B	55.4	65.6	71.1	60.1	-
Quato [23]	7B	55.7	65.9	71.9	59.0	-
ViLAMP [7]	7B	57.8	67.5	72.6	61.2	45.2
LLaVA-Video [47]	7B	52.9	64.4	68.6	58.2	43.1
+ FlexSelect	7B	59.8 ↑6.9	68.9 ↑4.5	73.2 ↑4.6	61.9 ↑3.7	52.9 ↑9.8
+ FlexSelect-Lite	7B	58.3 ↑5.4	68.3 ↑3.9	71.8 ↑3.2	60.7 ↑2.5	52.2 ↑9.1
InternVL2.5 [6]	8B	52.8	64.2	68.9	59.5	43.4
+ FlexSelect	8B	58.1 ↑5.3	67.0 ↑2.8	71.9 ↑3.0	60.1 ↑0.6	49.7 ↑6.3
+ FlexSelect-Lite	8B	57.9 ↑5.1	67.2 ↑3.0	71.9 ↑3.0	61.2 ↑1.7	49.9 ↑6.5
Qwen2.5-VL [1]	7B	55.6	65.4	70.2	59.5	45.3
+ FlexSelect	7B	59.3 ↑3.7	68.2 ↑2.8	72.5 ↑2.3	62.4 ↑2.9	51.2 ↑5.9
+ FlexSelect-Lite	7B	58.6 ↑3.0	67.4 ↑2.0	70.3 ↑0.1	61.9 ↑2.4	50.0 ↑4.7
LLaVA-Video [47]	72B	61.9	70.0	71.2	62.4	45.5
+ FlexSelect	72B	66.1 ↑4.2	73.1 ↑3.1	76.0 ↑4.8	66.9 ↑4.5	55.5 ↑10.0
Qwen2.5 VL [1]	72B	63.9	73.4	76.3	66.2	47.3
+ FlexSelect	72B	66.9 ↑3.0	74.4 ↑1.0	76.6 ↑0.3	66.4 ↑0.2	56.6 ↑9.3

Table 1: Comprehensive evaluation on different long video benchmarks. Gray rows show baseline results reproduced from public model weights. FlexSelect employs attention scores from the reference layer in VideoLLM for token selection, while FlexSelect-Lite utilizes scores from our lightweight token selector. Our methods consistently improve performance when integrated into various VideoLLMs by selecting semantically relevant visual tokens from extensive sampled frames. The implementation details of these results can be found in appendix A.3.

Since the ranking operation (i.e. argsort) itself is non-differentiable, we adopt a differentiable sorting algorithm [2] to approximate ranks and enable gradient backpropagation. This ensures effective training while strictly supervising the model on ranking quality.

Integration into FlexSelect Pipeline At inference, the lightweight selector directly replaces the transformer layers from the bigger VideoLLM to process visual tokens and query inputs and produces semantic relevance scores, eliminating the need for intermediate VideoLLM computation. By using these scores to select only the top-ranking tokens, we significantly reduce computational overhead, enabling efficient long-video understanding at scale. For clarity, we denote the FlexSelect integrated with the lightweight token selector as FlexSelect-Lite.

4 Experiments

4.1 Models and Benchmarks

We conduct comprehensive evaluations across diverse VideoLLM architectures and scales to assess the generalizability of our FlexSelect, including: (1) LLaVA-Video (7B/72B) [47], (2) InternVL-2.5 8B [6], and (3) Qwen2.5VL (7B/72B) [1]. The models are evaluated on four established long-video understanding benchmarks: (1) LongVideoBench [36], a benchmark designed for accurate retrieval

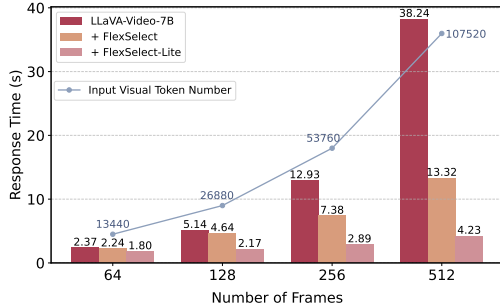


Figure 5: Response time when sampling different number of frames. FlexSelect accelerates inference by selecting semantically relevant visual tokens faithfully.

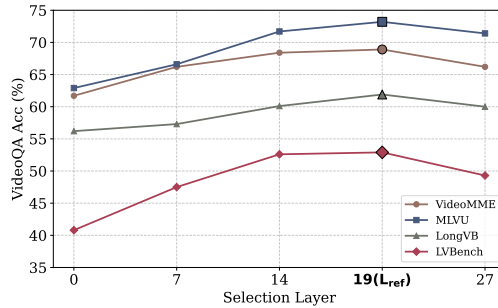


Figure 6: VideoQA Acc with different layers for token selection. The reference layer (19th) yields a more faithful cross-modal ranking for token selection.

and reasoning in long-context videos, we report the validation set result. (2) MLVU [48], a multitask benchmark specifically designed for long-form video understanding, we report the M-avg score. (3) VideoMME [11], a comprehensive evaluation across short/medium/long videos, we report the the long and overall results without subtitles. (4) LVBench [33], an extreme-long video benchmark with average video length reaches to one hour.

4.2 Main Results

Compared to SoTAs As shown in Table 1, our methods consistently enhance VideoLLM performance across multiple benchmarks. For LLaVA-Video-7B, FlexSelect delivers a +5.5 points improvements in average (+4.5 on VideoMME, +4.6 on MLVU, +3.7 on LongVB, and +9.8 on LVBench), surpassing other long-form video understanding methods like SF-LLaVA [38], TPO [17], Quato [23] and ViLAMP [7] at 7B parameter scale, demonstrating its effectiveness for long video understanding. FlexSelect-Lite maintains most of these gains (+3.9 in average) with less computational cost, validating the effectiveness of our rank-supervised token selector. The method’s adaptability is further confirmed by similar improvements when integrated into other models: Qwen2.5-VL-7B shows an average gain of +3.5 with FlexSelect and +2.3 with FlexSelect-Lite, while InternVL2.5-8B achieves an average improvement of +3.2 with FlexSelect and +3.7 with FlexSelect-Lite.

For larger-scale models, FlexSelect continues to deliver impressive results: LLaVA-Video-72B with FlexSelect shows a +4.5 improvement on LongVB (62.4 \rightarrow 66.9), outperforming GPT-4o (66.7). Qwen2.5VL-72B with FlexSelect sets new state-of-the-art results among open-source methods, achieving +9.3 on LVBench (47.3 \rightarrow 56.6). These consistent improvements across model sizes and benchmarks demonstrate the ability of FlexSelect to select semantically relevant tokens, confirming the effectiveness of our token selection mechanism.

Efficient Long Video Understanding Our method significantly improves VideoLLM’s efficiency when processing long videos with extensive frames. We evaluate the response time (i.e., time cost to generate the first token) on LLaVA-Video-7B. As shown in Figure 5, both FlexSelect and FlexSelect-Lite reduce response time for the same number of frames by decreasing the visual token number. FlexSelect-Lite achieves more pronounced acceleration, highlighting the efficiency of our lightweight token selector. This speed advantage grows progressively with more sampled frames: for 512 frames, LLaVA-Video-7B requires 38.24 s per sample, while FlexSelect-Lite reduces this to just 4.23 s—achieving a 9 \times speedup. More analysis on FLOPs estimation can be found in appendix A.2.

4.3 Ablations

Effectiveness of Reference Layer We compare the performance of FlexSelect on LLaVA-Video-7B when using attention scores from different layers for token selection. The evaluation is conducted with 512 input frames and 6,720 max selected tokens. As shown in Figure 6, the reference layer (layer 19) performs the best, as it can more accurately select semantically related tokens.

Input Frames	VideoMME (%)
64	65.2
128	67.8
256	68.1
512	68.9
1024	68.1

Max Selected Tokens	VideoMME (%)
1,680	67.1
3,360	68.4
6,720	68.9
13,440	68.1

Table 2: Ablation on input frames and max selected tokens of training-free FlexSelect. Evaluations are conducted on LLaVA-Video-7B.

Training Data Scale	VideoMME (%)
No training	61.9
1% (14k samples)	63.3
2% (29k samples)	63.4
5% (67k samples)	63.9
10% (134k samples)	63.5

Instruction Type	VideoMME (%)
Detail caption	63.5
Open-ended QA	63.6
Multi-choice QA	63.7
Mixed types	63.9

Table 3: Ablation on data scale and instruction type of rank-supervised training. Our token selector boosts performance while requiring only 5% of training data.

Influence of Input Frames and Max Selected Tokens We evaluate LLaVA-Video-7B with FlexSelect on VideoMME under varying input frames and max selected tokens. As demonstrated in Table 2, when fixing the max selected tokens to 6,720, we observe progressive accuracy improvements as the input frames increase from 64 to 512, followed by a slight degradation at 1,024 frames. Similarly, with input frames fixed at 512, performance improves when increasing max selected tokens from 1,680 to 6,720, but further selecting 13,440 tokens reduces the accuracy. The result shows that insufficient input frames or selected tokens cannot adequately cover the video content, risking overlook critical information, while excessive frames or tokens may introduce semantically irrelevant noise - both scenarios ultimately degrading performance.

Scales and Types of Training Data We train token selectors for LLaVA-Video-7B under different data scale and video instruction types, and evaluate them with 64 input frames and 1,680 max selected tokens. We first randomly sample 4 subsets (1%, 2%, 5%, 10%) from LLaVA-Video-178K [47] without considering video instruction type, using them as training datasets to train different token selectors. As shown in Table 3, directly initializing the token selector from a small-scale VideoLLM achieves an accuracy of 61.9%, while after training with just 1% of the data, the accuracy rises to 63.3%. The performance peaks when trained on 5% of the data (approximately 67k samples), and saturates with more data, demonstrating the quick convergence and training efficiency of our rank-supervised training. Subsequently, we fix the data scale at 67k samples while varying the video instruction types. Results show comparable performance across multiple-choice QA, open-ended QA, and video captioning data, suggesting that our training is effective on various instruction types.

Token Selector Params	Response Time	Datasets			
		VideoMME	LongVB	MLVU	LVBench
0.5 B	4.0 s	67.2	61.2	71.9	49.9
1.8 B	7.4 s	67.3	60.6	71.7	49.7
3.0 B	12.0 s	67.4	61.8	72.8	50.1

Table 4: Ablation on token selector parameters of rank-supervised training. We train different parameter size token selector for InternVL2.5-8B and test their accuracy on four benchmark. Evaluations are conducted with input frames set to 512 and max selected tokens set to 8,256.

Parameter Scale of Token Selector We investigate the impact of token selector parameter scale on performance. We train token selectors with 0.5B, 1.8B, and 3B parameters for InternVL2.5-8B, which are initialized from InternVL2.5-1B, InternVL2.5-2B and InternVL2.5-4B respectively, then we compare their performance on four benchmarks. Our results in Table 4 show that the 3B token selector achieves slightly higher scores than others but incurs significant computational overhead, and the 0.5B model delivers comparable performance while requiring only one-third of the response time of 3B model (4.0s vs. 12.0s). This indicates that scaling parameter of token selector brings limited gains, and 0.5B is a cost-effective choice.

5 Conclusion

This paper presents FlexSelect, a flexible and efficient token selection method that leverages cross-modal attention scores in VideoLLMs to identify query-relevant visual tokens. Our approach combines: (1) training-free attention-based token ranking, and (2) a lightweight selector for fast filtering. Its architecture-agnostic design enables integration into diverse VideoLLMs without modification. By selecting the most query-relevant visual tokens, FlexSelect achieves SoTA results on VideoMME (74.4), MLVU (76.6), LongVideoBench (66.9), and LVBench (56.6) while reducing tokens by over 90% (up to 9× speedup). This method demonstrates powerful long-form video understanding capabilities, enabling effective analysis of long-form videos with minimal computational overhead.

References

- [1] Shuai Bai, Keqin Chen, Xuejing Liu, Jialin Wang, Wenbin Ge, Siboz Song, Kai Dang, Peng Wang, Shijie Wang, Jun Tang, Humen Zhong, Yuanzhi Zhu, Mingkun Yang, Zhaohai Li, Jianqiang Wan, Pengfei Wang, Wei Ding, Zheren Fu, Yiheng Xu, Jiabo Ye, Xi Zhang, Tianbao Xie, Zesen Cheng, Hang Zhang, Zhibo Yang, Haiyang Xu, and Junyang Lin. Qwen2.5-vl technical report, 2025. URL <https://arxiv.org/abs/2502.13923>.
- [2] Mathieu Blondel, Olivier Teboul, Quentin Berthet, and Josip Djolonga. Fast differentiable sorting and ranking, 2020. URL <https://arxiv.org/abs/2002.08871>.
- [3] Rasmus Bro and Age K Smilde. Principal component analysis. *Analytical methods*, 6(9): 2812–2831, 2014.
- [4] Liang Chen, Haozhe Zhao, Tianyu Liu, Shuai Bai, Junyang Lin, Chang Zhou, and Baobao Chang. An image is worth 1/2 tokens after layer 2: Plug-and-play inference acceleration for large vision-language models, 2024. URL <https://arxiv.org/abs/2403.06764>.
- [5] Yukang Chen, Fuzhao Xue, Dacheng Li, Qinghao Hu, Ligeng Zhu, Xiuyu Li, Yunhao Fang, Haotian Tang, Shang Yang, Zhijian Liu, Ethan He, Hongxu Yin, Pavlo Molchanov, Jan Kautz, Linxi Fan, Yuke Zhu, Yao Lu, and Song Han. Longvila: Scaling long-context visual language models for long videos, 2024. URL <https://arxiv.org/abs/2408.10188>.
- [6] Zhe Chen, Weiyun Wang, Yue Cao, Yangzhou Liu, Zhangwei Gao, Erfei Cui, Jinguo Zhu, Shenglong Ye, Hao Tian, Zhaoyang Liu, Lixin Gu, Xuehui Wang, Qingyun Li, Yimin Ren, Zixuan Chen, Jiapeng Luo, Jiahao Wang, Tan Jiang, Bo Wang, Conghui He, Botian Shi, Xingcheng Zhang, Han Lv, Yi Wang, Wenqi Shao, Pei Chu, Zhongying Tu, Tong He, Zhiyong Wu, Huipeng Deng, Jiaye Ge, Kai Chen, Kaipeng Zhang, Limin Wang, Min Dou, Lewei Lu, Xizhou Zhu, Tong Lu, Dahua Lin, Yu Qiao, Jifeng Dai, and Wenhui Wang. Expanding performance boundaries of open-source multimodal models with model, data, and test-time scaling, 2025. URL <https://arxiv.org/abs/2412.05271>.
- [7] Chuanqi Cheng, Jian Guan, Wei Wu, and Rui Yan. Scaling video-language models to 10k frames via hierarchical differential distillation, 2025. URL <https://arxiv.org/abs/2504.02438>.
- [8] Anxhelo Diko, Tinghui Wang, Wassim Swaileh, Shiyun Sun, and Ioannis Patras. Rewind: Understanding long videos with instructed learnable memory, 2025. URL <https://arxiv.org/abs/2411.15556>.
- [9] Mark Endo, Xiaohan Wang, and Serena Yeung-Levy. Feather the throttle: Revisiting visual token pruning for vision-language model acceleration, 2024. URL <https://arxiv.org/abs/2412.13180>.
- [10] Jiajun Fei, Dian Li, Zhidong Deng, Zekun Wang, Gang Liu, and Hui Wang. Video-ccam: Enhancing video-language understanding with causal cross-attention masks for short and long videos, 2024. URL <https://arxiv.org/abs/2408.14023>.
- [11] Chaoyou Fu, Yuhao Dai, Yongdong Luo, Lei Li, Shuhuai Ren, Renrui Zhang, Zihan Wang, Chenyu Zhou, Yunhang Shen, Mengdan Zhang, Peixian Chen, Yanwei Li, Shaohui Lin, Sirui Zhao, Ke Li, Tong Xu, Xiawu Zheng, Enhong Chen, Rongrong Ji, and Xing Sun. Video-mme: The first-ever comprehensive evaluation benchmark of multi-modal llms in video analysis, 2024. URL <https://arxiv.org/abs/2405.21075>.

- [12] Tianyu Fu, Tengxuan Liu, Qinghao Han, Guohao Dai, Shengen Yan, Huazhong Yang, Xuefei Ning, and Yu Wang. Framefusion: Combining similarity and importance for video token reduction on large visual language models, 2024. URL <https://arxiv.org/abs/2501.01986>.
- [13] Lishuai Gao, Yujie Zhong, Yingsen Zeng, Haoxian Tan, Dengjie Li, and Zheng Zhao. Linvt: Empower your image-level large language model to understand videos, 2024. URL <https://arxiv.org/abs/2412.05185>.
- [14] Bo Li, Yuanhan Zhang, Dong Guo, Renrui Zhang, Feng Li, Hao Zhang, Kaichen Zhang, Peiyuan Zhang, Yanwei Li, Ziwei Liu, and Chunyuan Li. Llava-onevision: Easy visual task transfer, 2024. URL <https://arxiv.org/abs/2408.03326>.
- [15] Dongxu Li, Yudong Liu, Haoning Wu, Yue Wang, Zhiqi Shen, Bowen Qu, Xinyao Niu, Fan Zhou, Chengen Huang, Yanpeng Li, Chongyan Zhu, Xiaoyi Ren, Chao Li, Yifan Ye, Peng Liu, Lihuan Zhang, Hanshu Yan, Guoyin Wang, Bei Chen, and Junnan Li. Aria: An open multimodal native mixture-of-experts model, 2025. URL <https://arxiv.org/abs/2410.05993>.
- [16] Junnan Li, Dongxu Li, Silvio Savarese, and Steven Hoi. Blip-2: Bootstrapping language-image pre-training with frozen image encoders and large language models. In *International conference on machine learning*, pages 19730–19742. PMLR, 2023.
- [17] Rui Li, Xiaohan Wang, Yuhui Zhang, Zeyu Wang, and Serena Yeung-Levy. Temporal preference optimization for long-form video understanding, 2025. URL <https://arxiv.org/abs/2501.13919>.
- [18] Yanwei Li, Chengyao Wang, and Jiaya Jia. Llama-vid: An image is worth 2 tokens in large language models, 2023. URL <https://arxiv.org/abs/2311.17043>.
- [19] Jiajun Liu, Yibing Wang, Hanghang Ma, Xiaoping Wu, Xiaoqi Ma, Xiaoming Wei, Jianbin Jiao, Enhua Wu, and Jie Hu. Kangaroo: A powerful video-language model supporting long-context video input, 2024. URL <https://arxiv.org/abs/2408.15542>.
- [20] Xiangrui Liu, Yan Shu, Zheng Liu, Ao Li, Yang Tian, and Bo Zhao. Video-xl-pro: Reconstructive token compression for extremely long video understanding, 2025. URL <https://arxiv.org/abs/2503.18478>.
- [21] Zhijian Liu, Ligeng Zhu, Baifeng Shi, Zhuoyang Zhang, Yuming Lou, Shang Yang, Haocheng Xi, Shiyi Cao, Yuxian Gu, Dacheng Li, Xiuyu Li, Yunhao Fang, Yukang Chen, Cheng-Yu Hsieh, De-An Huang, An-Chieh Cheng, Vishwesh Nath, Jinyi Hu, Sifei Liu, Ranjay Krishna, Daguang Xu, Xiaolong Wang, Pavlo Molchanov, Jan Kautz, Hongxu Yin, Song Han, and Yao Lu. Nvila: Efficient frontier visual language models, 2025. URL <https://arxiv.org/abs/2412.04468>.
- [22] Zuyan Liu, Yuhao Dong, Ziwei Liu, Winston Hu, Jiwen Lu, and Yongming Rao. Oryx mllm: On-demand spatial-temporal understanding at arbitrary resolution, 2025. URL <https://arxiv.org/abs/2409.12961>.
- [23] Yongdong Luo, Wang Chen, Xiawu Zheng, Weizhong Huang, Shukang Yin, Haojia Lin, Chaoyou Fu, Jinfa Huang, Jiayi Ji, Jiebo Luo, and Rongrong Ji. Quota: Query-oriented token assignment via cot query decouple for long video comprehension, 2025. URL <https://arxiv.org/abs/2503.08689>.
- [24] OpenAI. Hello GPT-4o, 5 2024. URL <https://openai.com/index/hello-gpt-4o/>. Accessed: 2024-05-20.
- [25] Bowen Peng, Jeffrey Quesnelle, Honglu Fan, and Enrico Shippole. Yarn: Efficient context window extension of large language models, 2023. URL <https://arxiv.org/abs/2309.00071>.
- [26] Yujia Qin, Yining Ye, Junjie Fang, Haoming Wang, Shihao Liang, Shizuo Tian, Junda Zhang, Jiahao Li, Yunxin Li, Shijue Huang, Wanjun Zhong, Kuanye Li, Jiale Yang, Yu Miao, Woyu Lin, Longxiang Liu, Xu Jiang, Qianli Ma, Jingyu Li, Xiaojun Xiao, Kai Cai, Chuang Li, Yaowei

- Zheng, Chaolin Jin, Chen Li, Xiao Zhou, Minchao Wang, Haoli Chen, Zhaojian Li, Haihua Yang, Haifeng Liu, Feng Lin, Tao Peng, Xin Liu, and Guang Shi. Ui-tars: Pioneering automated gui interaction with native agents, 2025. URL <https://arxiv.org/abs/2501.12326>.
- [27] Yan Shu, Zheng Liu, Peitian Zhang, Minghao Qin, Junjie Zhou, Zhengyang Liang, Tiejun Huang, and Bo Zhao. Video-xl: Extra-long vision language model for hour-scale video understanding, 2024. URL <https://arxiv.org/abs/2409.14485>.
- [28] Charles Spearman. The proof and measurement of association between two things. In James J. Jenkins and Donald G. Paterson, editors, *Studies in Individual Differences: The Search for Intelligence*, pages 45–58. Appleton-Century-Crofts, 1961. doi: 10.1037/11491-005. URL <https://doi.org/10.1037/11491-005>.
- [29] Keda Tao, Can Qin, Haoxuan You, Yang Sui, and Huan Wang. Dycoke: Dynamic compression of tokens for fast video large language models, 2025. URL <https://arxiv.org/abs/2411.15024>.
- [30] Gemini Team, Rohan Anil, Sebastian Borgeaud, Jean-Baptiste Alayrac, Jiahui Yu, Radu Soricut, Johan Schalkwyk, Andrew M. Dai, Anja Hauth, and et al. Gemini: A family of highly capable multimodal models, 2024. URL <https://arxiv.org/abs/2312.11805>.
- [31] Qwen Team, An Yang, Baosong Yang, Beichen Zhang, Binyuan Hui, Bo Zheng, Bowen Yu, Chengyuan Li, Dayiheng Liu, Fei Huang, Haoran Wei, Huan Lin, Jian Yang, Jianhong Tu, Jianwei Zhang, Jianxin Yang, Jiayi Yang, Jingren Zhou, Junyang Lin, Kai Dang, Keming Lu, Keqin Bao, Kexin Yang, Le Yu, Mei Li, Mingfeng Xue, Pei Zhang, Qin Zhu, Rui Men, Runji Lin, Tianhao Li, Tianyi Tang, Tingyu Xia, Xingzhang Ren, Xuancheng Ren, Yang Fan, Yang Su, Yichang Zhang, Yu Wan, Yuqiong Liu, Zeyu Cui, Zhenru Zhang, and Zihan Qiu. Qwen2.5 technical report, 2025. URL <https://arxiv.org/abs/2412.15115>.
- [32] Peng Wang, Shuai Bai, Sinan Tan, Shijie Wang, Zhihao Fan, Jinze Bai, Keqin Chen, Xuejing Liu, Jialin Wang, Wenbin Ge, Yang Fan, Kai Dang, Mengfei Du, Xuancheng Ren, Rui Men, Dayiheng Liu, Chang Zhou, Jingren Zhou, and Junyang Lin. Qwen2-vl: Enhancing vision-language model’s perception of the world at any resolution, 2024. URL <https://arxiv.org/abs/2409.12191>.
- [33] Weihang Wang, Zehai He, Wenyi Hong, Yean Cheng, Xiaohan Zhang, Ji Qi, Xiaotao Gu, Shiyu Huang, Bin Xu, Yuxiao Dong, Ming Ding, and Jie Tang. Lvbench: An extreme long video understanding benchmark, 2024. URL <https://arxiv.org/abs/2406.08035>.
- [34] Xiao Wang, Qingyi Si, Jianlong Wu, Shiyu Zhu, Li Cao, and Liqiang Nie. Adaretake: Adaptive redundancy reduction to perceive longer for video-language understanding, 2025. URL <https://arxiv.org/abs/2503.12559>.
- [35] Zichen Wen, Yifeng Gao, Shaobo Wang, Junyuan Zhang, Qintong Zhang, Weijia Li, Conghui He, and Linfeng Zhang. Stop looking for important tokens in multimodal language models: Duplication matters more, 2025. URL <https://arxiv.org/abs/2502.11494>.
- [36] Haoning Wu, Dongxu Li, Bei Chen, and Junnan Li. Longvideobench: A benchmark for long-context interleaved video-language understanding, 2024. URL <https://arxiv.org/abs/2407.15754>.
- [37] Long Xing, Qidong Huang, Xiaoyi Dong, Jiajie Lu, Pan Zhang, Yuhang Zang, Yuhang Cao, Conghui He, Jiaqi Wang, Feng Wu, and Dahua Lin. Pyramidrop: Accelerating your large vision-language models via pyramid visual redundancy reduction, 2025. URL <https://arxiv.org/abs/2410.17247>.
- [38] Mingze Xu, Mingfei Gao, Shiyu Li, Jiasen Lu, Zhe Gan, Zhengfeng Lai, Meng Cao, Kai Kang, Yinfei Yang, and Afshin Dehghan. Slowfast-llava-1.5: A family of token-efficient video large language models for long-form video understanding, 2025. URL <https://arxiv.org/abs/2503.18943>.
- [39] Jiabo Ye, Haiyang Xu, Haowei Liu, Anwen Hu, Ming Yan, Qi Qian, Ji Zhang, Fei Huang, and Jingren Zhou. mplug-owl3: Towards long image-sequence understanding in multi-modal large language models, 2024. URL <https://arxiv.org/abs/2408.04840>.

- [40] Boqiang Zhang, Kehan Li, Zesen Cheng, Zhiqiang Hu, Yuqian Yuan, Guanzheng Chen, Sicong Leng, Yuming Jiang, Hang Zhang, Xin Li, Peng Jin, Wenqi Zhang, Fan Wang, Lidong Bing, and Deli Zhao. Videollama 3: Frontier multimodal foundation models for image and video understanding, 2025. URL <https://arxiv.org/abs/2501.13106>.
- [41] Boqiang Zhang, Kehan Li, Zesen Cheng, Zhiqiang Hu, Yuqian Yuan, Guanzheng Chen, Sicong Leng, Yuming Jiang, Hang Zhang, Xin Li, Peng Jin, Wenqi Zhang, Fan Wang, Lidong Bing, and Deli Zhao. Videollama 3: Frontier multimodal foundation models for image and video understanding, 2025. URL <https://arxiv.org/abs/2501.13106>.
- [42] Kaichen Zhang, Bo Li, Peiyuan Zhang, Fanyi Pu, Joshua Adrian Cahyono, Kairui Hu, Shuai Liu, Yuanhan Zhang, Jingkang Yang, Chunyuan Li, and Ziwei Liu. Lmms-eval: Reality check on the evaluation of large multimodal models, 2024. URL <https://arxiv.org/abs/2407.12772>.
- [43] Peiyuan Zhang, Kaichen Zhang, Bo Li, Guangtao Zeng, Jingkang Yang, Yuanhan Zhang, Ziyue Wang, Haoran Tan, Chunyuan Li, and Ziwei Liu. Long context transfer from language to vision, 2024. URL <https://arxiv.org/abs/2406.16852>.
- [44] Qizhe Zhang, Aosong Cheng, Ming Lu, Zhiyong Zhuo, Minqi Wang, Jiajun Cao, Shaobo Guo, Qi She, and Shanghang Zhang. [cls] attention is all you need for training-free visual token pruning: Make vlm inference faster, 2024. URL <https://arxiv.org/abs/2412.01818>.
- [45] Shaolei Zhang, Qingkai Fang, Zhe Yang, and Yang Feng. Llava-mini: Efficient image and video large multimodal models with one vision token. *arXiv preprint arXiv:2501.03895*, 2025.
- [46] Yuan Zhang, Chun-Kai Fan, Junpeng Ma, Wenzhao Zheng, Tao Huang, Kuan Cheng, Denis Gudovskiy, Tomoyuki Okuno, Yohei Nakata, Kurt Keutzer, and Shanghang Zhang. Sparsevlm: Visual token sparsification for efficient vision-language model inference, 2025. URL <https://arxiv.org/abs/2410.04417>.
- [47] Yuanhan Zhang, Jinming Wu, Wei Li, Bo Li, Zejun Ma, Ziwei Liu, and Chunyuan Li. Video instruction tuning with synthetic data, 2024. URL <https://arxiv.org/abs/2410.02713>.
- [48] Junjie Zhou, Yan Shu, Bo Zhao, Boya Wu, Zhengyang Liang, Shitao Xiao, Minghao Qin, Xi Yang, Yongping Xiong, Bo Zhang, Tiejun Huang, and Zheng Liu. Mlvu: Benchmarking multi-task long video understanding, 2025. URL <https://arxiv.org/abs/2406.04264>.
- [49] Orr Zohar, Xiaohan Wang, Yann Dubois, Nikhil Mehta, Tong Xiao, Philippe Hansen-Estruch, Licheng Yu, Xiaofang Wang, Felix Juefei-Xu, Ning Zhang, Serena Yeung-Levy, and Xide Xia. Apollo: An exploration of video understanding in large multimodal models, 2024. URL <https://arxiv.org/abs/2412.10360>.

A Appendix / supplemental material

A.1 Details of Recall@K Experiment

Needle Images and Queries The needle images and corresponding queries used in our Recall@K experiment are directly borrowed from the V-NIAH experiment in LongVA [43], which provides five needle-query pairs. We randomly sample 128 videos from the VideoMME [11] test set and insert each needle-query pair into them, resulting in a total of 640 test samples. We compute Recall@K on these samples.

Recall@K of Various Models In addition to LLaVA-Video-7B, we calculate Recall@K for LLaVA-Video-72B, InternVL2.5-8B, Qwen2.5VL-7B and Qwen2.5VL-72B. The result is shown at Figure 7. We identify the reference layer of these models: layer 15 for InternVL2.5-8B, layer 60 for LLaVA-Video-7B, layer 20 for Qwen2.5VL-7B and layer 60 for Qwen2.5VL-72B.

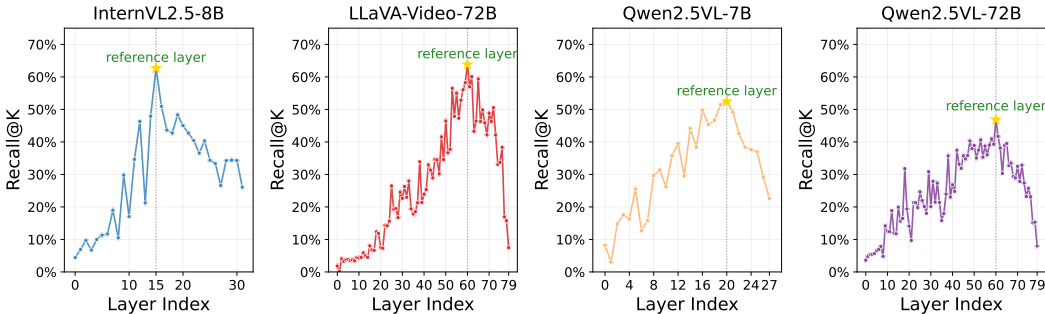


Figure 7: Recall@K across layers of different VideoLLMs.

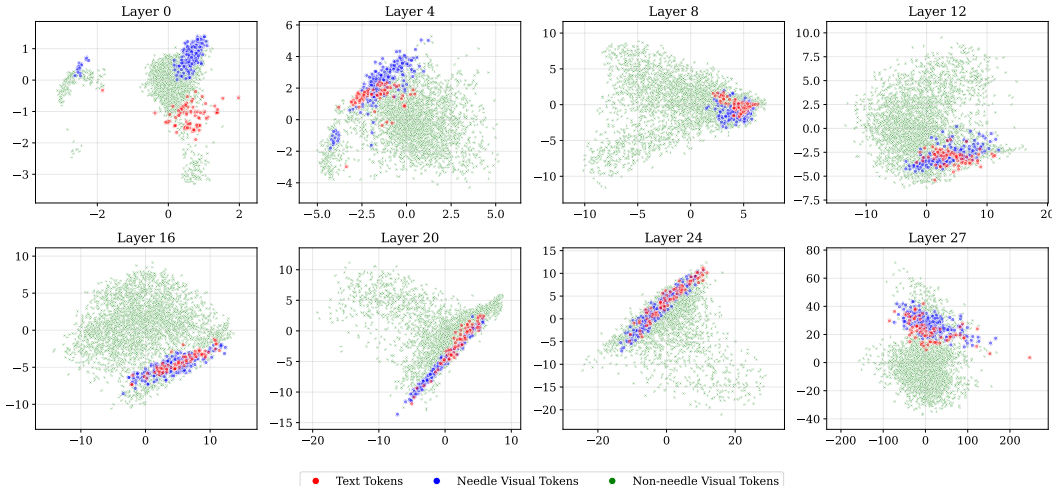


Figure 8: PCA visualization of query tokens, needle visual tokens (i.e. semantically related tokens) and non-needle visual tokens from different layers of LLaVA-Video-7B. We found that the correlation between distributions of text tokens and needle visual tokens varies with layer depth, matching the trend of Recall@K: at shallow layers, their distributions diverge; in intermediate layers, a strong linear correlation emerges; while at very deep layers, this linear correlation weakens. This finding demonstrates that semantic alignment between visual and text tokens established at intermediate layers in VideoLLMs, which further explains the emergence of the reference layer.

PCA Visualization We further visualize the query tokens, needle visual tokens and non-needle visual tokens using Principal Component Analysis (PCA) [3] to examine cross-modal semantic alignment across different layers in VideoLLMs. As shown in Figure 8 (LLaVA-Video-7B), a

significant distribution discrepancy exists between text tokens and needle visual tokens in shallow layers. As the layer depth increases, these distributions develop a strong linear correlation in deeper layers, which subsequently weakens in the deepest layers. This indicates that the cross-modal semantic alignment is initially absent in early layers, gradually strengthens in intermediate layers, and then decreases in the final layers, which is consistent with the trend of Recall@K.

A.2 FLOPs Analysis

Suppose the transformer decoder of VideoLLM has L layers, h heads, and the hidden states size is d , the intermediate size of FFN is m . For an input sequence of n tokens, the FLOPs of the prefilling stage can be estimated as:

$$\text{FLOPs} = L \times (4nd^2 + 2n^2d + 2ndm) \approx 2Ln^2d,$$

since $n \gg d$ and $n \gg m$ in typical scenarios.

When using FlexSelect, assuming the M -th layer serves as the reference layer and the input sequence is partitioned into K segments via our frame set partition operation, ultimately selecting n' tokens, the FLOPs can be estimated as:

$$\text{FLOPs}' = M \times (4nd^2 + \frac{2n^2d}{K} + 2ndm) + L \times (4n'd^2 + 2n'^2d + 2n'dm) \approx \frac{2Mn^2d}{K},$$

since in our configuration, $n' = 0.0625n$, making the $L \times (4n'd^2 + 2n'^2d + 2n'dm)$ term negligible in FLOPs'. Consequently, FlexSelect requires only $\frac{M}{L} \times \frac{1}{K}$ of the original FLOPs.

Similarly, when employing FlexSelect-Lite, the Flops can be estimated as $\frac{2L'n'^2d'}{K}$, where L' and d' are layer num and hidden states dimension of lightweight token selector. This FLOPs is more smaller than FlexSelect because $L' < L$ and $d' < d$. FLOPs estimation only provides a theoretical reference for computational cost. For practical considerations, we recommend referring to the actual time cost analysis in Figure 5.

A.3 Implementation Details

The evaluations in main Table 1 are conducted under LMMS-Eval [42] framework on 8 96G H20 GPUs. We set the input frames number N to 1024, 512, 512 for Qwen2.5VL(7B/72B), LLaVA-Video(7B/72B), and InternVL2.5-8B respectively, and max subset frames number S to 64 for all models. Denoting N_{image} is the token number required for encoding one frame, we select 7,010 ($64 * N_{\text{image}}$), 6,720 ($32 * N_{\text{image}}$), 8,256 ($32 * N_{\text{image}}$) visual tokens for these models respectively, which is 6.25% of original input length. The reference layer L for token selection are set to Layer 15 for InternVL2.5-8B, Layer 19 for LLaVA-Video-7B, Layer 20 for Qwen2.5VL-7B, Layer 60 for LLaVA-Video-72B and Qwen2.5VL-72B determined by $\arg \max_L \text{Recall}@K(L)$.

We train lightweight token selectors for 7B/8B models but exclude 72B due to memory constraints. For token selector of LLaVA-Video-7B, we initialize it with the decoder of LLaVA-OneVision-0.5B [14]; for token selector of InternVL2.5-8B, we initialize it with the decoder of InternVL-1B. In the case of Qwen2.5VL-7B, where no similarly-sized VideoLLM is available, we directly initialize it with Qwen2.5-Instruct-0.5B [31]. We randomly select a small (5%) subset of LLaVA-Video-178K [47] as the training data, which contains about 67k video instruction samples. We uniformly sample 64 frames from each video during selector training. Token selectors for LLaVA-Video and InternVL2.5 were trained for 1 epoch, while the token selector for Qwen2.5VL was trained for 3 epochs since it was initialized from a language model, which is lack of visual prior knowledge, and requires more training steps to achieve convergence.

A.4 Limitations

FlexSelect enhances VideoLLMs' long-video understanding by selecting semantically relevant tokens, without modifying or retraining the base VideoLLM. Thus, its performance ceiling is bounded by the host VideoLLM's native capabilities. FlexSelect-Lite trains a lightweight token selector to predict the reference layer's importance scores in large-scale VideoLLMs. While more efficient, it typically underperforms direct reference-layer token selection. Nevertheless, compared to other heavily trained alternatives and existing sub-optimal token pruning methods, FlexSelect remains an efficient and effective solution for boosting diverse VideoLLMs' long-video comprehension.

A.5 Social Impacts

FlexSelect operates as a preprocessing module that selects semantically relevant visual tokens for diverse VideoLLMs. It is important to note that this method cannot prevent the base VideoLLMs from potentially generating erroneous, biased, or harmful hallucinations. When integrating FlexSelect with different VideoLLMs, users should be aware of and mitigate potential risks in the generated content.

A.6 Visualization of Some Examples

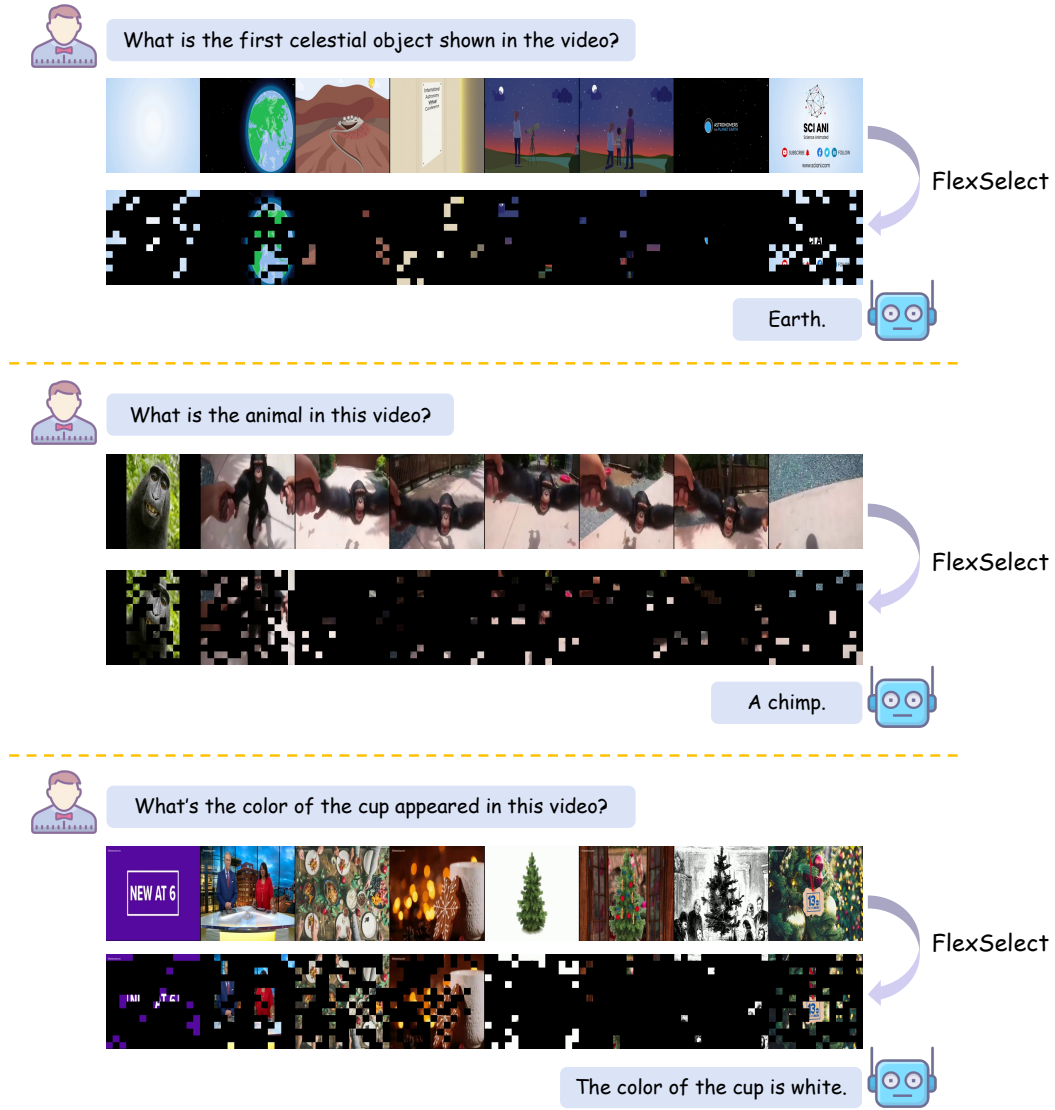


Figure 9: Some token selection examples of our FlexSelect on LLaVA-Video-7B. We choose 8 frames from the sampled frames for visualization.